



# Local positioning system for autonomous vertical take-off and landing using ultra-wide band measurement ranging system

Niam Tamami<sup>\*</sup>, Bambang Sumantri, Prima Kristalina

*Electrical Engineering Department, Politeknik Elektronika Negeri Surabaya  
Jl Raya ITS – Kampus PENS, Surabaya, 60111, Indonesia*

Received 27 November 2020; Accepted 20 May 2021; Published online 31 July 2021

## Abstract

An autonomous vertical take-off and landing (VTOL) must be supported with an accurate positioning system, especially for autonomous take-off, landing, and other tasks in small area. This paper presents a novel method of small local outdoor positioning system for localizing the area of dropping and landing of autonomous VTOL by utilizing the low-cost precision ultra-wide band (UWB) ranging system. We compared symmetrical single sided-two way ranging (SSS-TWR), symmetrical double sided-two way ranging (SDS-TWR), and asymmetrical double sided-two way ranging (ADS-TWR) methods to get precision ranging measurement on UWB radio module. ADS-TWR was superior to others by resulting in minimum distance error. The ADS-TWR average error was 1.38 % (35.88 cm), SDS-TWR average error was 1.83 % (47.58 cm), and SSS-TWR average error was 2.73 % (70.98 cm). Furthermore, the trilateration method was utilized to obtain the local position of the autonomous VTOL. The trilateration method successfully implemented autonomous VTOL quadcopter positioning in a small local outdoor area (20 m x 30 m). Autonomous VTOL has been able to drop seven payloads in seven areas (2 m x 2 m) and landed in the home position (3 m x 3 m) successfully.

©2021 Research Center for Electrical Power and Mechatronics - Indonesian Institute of Sciences. This is an open access article under the CC BY-NC-SA license (<https://creativecommons.org/licenses/by-nc-sa/4.0/>).

Keywords: autonomous VTOL; UWB local positioning system; trilateration.

## I. Introduction

The development of autonomous VTOL vehicle increases over this decade. This vehicle has many advantages over the other types because it is able to carry a heavy payload, easy to control, more stable, and has vertical take-off and landing ability. Therefore, this vehicle is widely used to facilitate human tasks. Some examples of using this vehicle are environmental mapping, human surveillance, and packet delivery.

Positioning ability is one most important capability in an autonomous VTOL system. The positioning system must be accurate to support take-off, hover, and landing in a safe area. Commonly, autonomous VTOL uses global positioning system (GPS) as a satellite-based positioning system. Usually, a GPS chip only has  $\pm 3$  m maximum accuracy based on the received signal from satellites. Autonomous VTOL is

complicated to take-off, hover or land in a narrower area. Therefore, autonomous VTOL requires accurate positioning. For example, environmental mapping autonomous VTOL requires precise positioning to avoid plotting mistake on the map. Another example is packet delivery autonomous VTOL. It requires accurate positioning to send the package to a specific home address and to drop it in the right and safe place, not in a random place in a home radius location.

There were some researches about UWB range measurement. Akahori *et al.* designed an indoor position estimation system with UWB, inertial measurement unit (IMU) and a distance sensor for quadcopter [1]. This system consisted of one tag and three anchor UWB modules. Quadcopter coordinates were calculated by the Pythagorean and extended Kalman filter equations. The maximum error for x, y coordinates were 0.2 m. Mai *et al.* developed an indoor local positioning estimator for unmanned blimp [2]. This system used UWB and gyroscope because GPS and magnetometer cannot work for indoor positioning. This system used a Kalman filter to estimate the state of the blimp. Experimental

<sup>\*</sup> Corresponding Author. Tel: +62-812-1796-6299  
E-mail address: [niam@pens.ac.id](mailto:niam@pens.ac.id)

results showed that the error estimator was less than 1 m and orientation error was less than 11 degrees. Ledergerber *et al.* developed a method for calibrating away inaccuracies in ultra-wideband range measurements using a maximum likelihood approach to minimize data error due to unideal antenna and environmental influence [3]. The research only used two UWB radio and tested in simulation by considering the only parameter of the UWB radio model without including the environmental condition. Guosheng *et al.* used extended Kalman filter and unscented Kalman filter to improve UWB system accuracy [4]. This system was used for mobile robot positioning. The experiments were carried out under non-line-of-sight (NLOS) and line-of-sight (LOS) conditions. Experiment result has shown that unscented Kalman filter has a smaller average error than extended Kalman filter. Feng *et al.* combined UWB and IMU to make an indoor navigation system [5]. They compared extended Kalman filter with least square and unscented Kalman filter with direct positioning algorithm to get the best-improved accuracy method. Experimental results showed that extended Kalman filter was better than least square, and unscented Kalman filter was better than direct positioning algorithm. Ren *et al.* developed a cow monitoring activity system using UWB and video processing [6]. They used seven UWB anchor and a UWB tag installed on a cow. The cow position was calculated using least square estimation (LSE) based UWB ranging data. This system has accuracy with mean error of 0.39 m and standard deviation of 0.62 m.

Several other kinds of research were bluetooth, Xbee, and radio frequency identification (RFID) localization system. However, these researches were only able to be used in areas under 10 m x 10 m. Ramadhani *et al.* developed an indoor localization system utilizing bluetooth low energy (BLE) [7]. They compared trilateration, trilateration-geometric dilution of precision (GDOP), multilateration, and multilateration-GDOP to localize the area. Multilateration-GDOP was superior to others. Giuliano *et al.* developed bluetooth low energy localization system [8]. Feed-forward Neural Network combined by Non-Linear Least Square Algorithm was used to calculate position estimation with 1 m accuracy. Pusnik *et al.* developed bluetooth low energy localization system [9]. This system detected the closest transmitter based on the data from previous measurements. Cheng *et al.* developed a book localization system in a bookshelf based RFID RSSI [10]. The distance between tag and anchor (antenna) was 38.5 cm. They used the deep learning method to estimate book position, and the average error is 10.02 cm. Ainul *et al.* developed an indoor mobile cooperative tracking system [11]. They used Xbee S2 pro module to get received signal strength indication (RSSI) data and to calculate the position by trilateration method. They also implemented extended gradient filter, extended Kalman filter and modified extended Kalman filter to improve localizing accuracy. Modified extended Kalman filter improved 41.28 % of accuracy.

Another technology used the WIFI localization system. The researches used RSSI to estimate distance. However, the RSSI data are not linear, depending on environmental conditions. Zhang *et al.* developed a hierarchical classification-based method to estimate position based WIFI received signal strength data [12]. This method offers 10 % to 22 % reduced average position error compared to several benchmark methods. Ashraf *et al.* used a Deep Neural Network Ensemble Classifier method to estimate position using WIFI RSSI [13]. This method showed mean error of 2.84 m with standard deviation of 2.24 m. Monica *et al.* developed a localization algorithm based on nonlinear programming [14]. This method was compared by particle swarm optimization and two-stage maximum likelihood. This method gave a guaranteed globally optimal solution of position estimation. Ssekidde *et al.* compared convolutional Neural Network and artificial Neural Network to identify a room [15]. They used WIFI RSSI data that were processed by continuous wavelet transforms. The experimental result showed that CNN superiors to ANN, with accuracies of 97.3 % and 70.6 % for CNN and ANN. Li *et al.* developed smartphone-based indoor localization [16]. They integrated channel state information (CSI) and magnetic field strength (MFS) localization methods. The experimental results showed that the mean distance error was less than 0.5 m. Koike-Akino *et al.* developed indoor localization using WIFI signal to noise ratio [17]. They used deep learning to calculate position. The position root mean square error is 28.7 cm in 250 cm x 350 cm area. Peng *et al.* developed an improved K-Nearest neighbor algorithm for indoor localization [18]. Compared with the KNN, E-WKNN, and P-WKNN algorithms, the positioning accuracy of this method was improved by 29.4 %, 23.5 %, and 20.7 %, respectively. Maghdid *et al.* developed an indoor localization simulation. They used long short-term memory recurrent Neural Network to estimate position based WIFI RSSI [19]. They improved the performance of long short-term memory recurrent Neural Network by adding a transfer learning algorithm to WIFI RSSI data. This simulation result confirmed that this method could obtain 1.5 m to 2 m positioning accuracy. Sadowski *et al.* compared KNN and Naive Bayes to calculate a tag position in a room [20]. The experiment showed that KNN is superior to Naive Bayes.

There were other researches about localization. Ranade *et al.* developed quadcopter obstacle avoidance and path planning simulation using the Flood Fill method [21]. This method was compared with the Potential Field method to show the fastest execution method. The result has been demonstrated that flood fills faster than the potential field method. Honig *et al.* developed quadcopter swarm trajectory planning for an indoor area using VICON camera positioning [22]. Shen *et al.* developed a cooperative relative navigation method that exploited ranging sensor to assist the global navigation satellite system (GNSS) [23]. This method improved navigation accuracy and robustness. Gu *et al.* developed Landmark Graph-based Indoor

Localization [24]. They used multisensory data on a smartphone (accelerometer, gyroscope, magnetometer, barometer, WIFI, light sensor) then extracted the feature to make a landmark on a building. This method has 0.8 m mean error. Ashraf *et al.* developed an indoor localization system using a convolutional Neural Network-based magnetic field pattern [25]. This system offered 1.01 m accuracy.

This paper presents a novel method of small local outdoor positioning system for localizing the area for dropping and landing of an autonomous VTOL, based on low-cost precision Ultra-Wide Band measurement ranging system.

## II. Materials and Methods

We started by designing ranging hardware. A set of UWB radio module was used to make small local positioning area for autonomous VTOL dropping or landing area. When autonomous VTOL did not detect UWB signal, GPS system was used. Autonomous VTOL went to small local positioning area using GPS coordinate and then detected UWB signal. When it was detected, local positioning process was started. Autonomous VTOL could drop or land in small local positioning area precisely.

Figure 1 shows a small local outdoor positioning area of autonomous VTOL. The area size is 20.00 m x 30.00 m. This system consists of autonomous VTOL and UWB tag (moveable position), and UWB anchor (fix position). UWB Anchor 1 is located at (11.00, 0.00) m, UWB Anchor 2 is located at (0, 15.00) m and UWB Anchor 3 is located at (11.00, 30.00) m. Autonomous VTOL can localize its position in this small local positioning area. Home area is 3 m x 3 m to take-off and landing operation, dropping area (yellow square) is 2 m x 2 m to drop user payloads. Home location position (red square) is (1.50, 1.50) m, and dropping positions (yellow square) are (8.50, 11.00), (1.00, 15.00), (4.00, 22.5), (1.00, 28.00), (18.50, 26.00), (12.50, 20.00), (17.00, 7.50) m.

### A. Software tag and anchor hardware design

This section presents about schematic design of UWB tag and anchor transceiver for ranging sensor. Figure 2 shows the schematic of UWB tag and anchor transceiver. We use DWM1000 as UWB IC chip and Arduino pro mini as main controller. Arduino gets ranging data from DWM1000 using SPI communication. SPICLK, SPIMISO, SPIMOSI, SPICS of UWB is connected respectively on D13, D12, D11, D10 Arduino pin. The system needs 3.3V so we add 3.3V voltage regulator IC. We also add led power indicator.

Figure 3 shows the hardware board for the tag and anchor transceiver from Figure 2 schematic. The green board is DWM1000, and the blue board is Arduino minimum system. This hardware board was duplicated into four pieces. One-piece as UWB Tag, the other as UWB anchor 1, UWB anchor 2, UWB anchor 3.

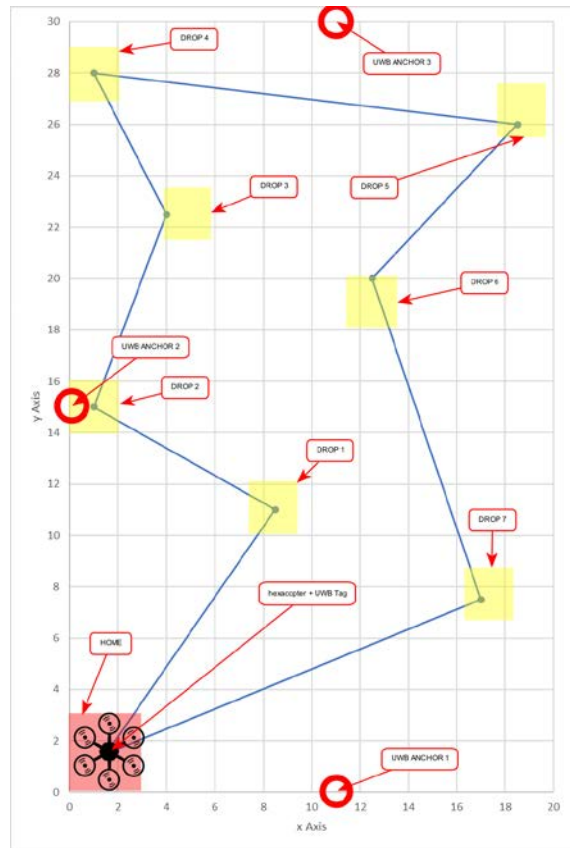


Figure 1. A small local outdoor positioning area of autonomous VTOL

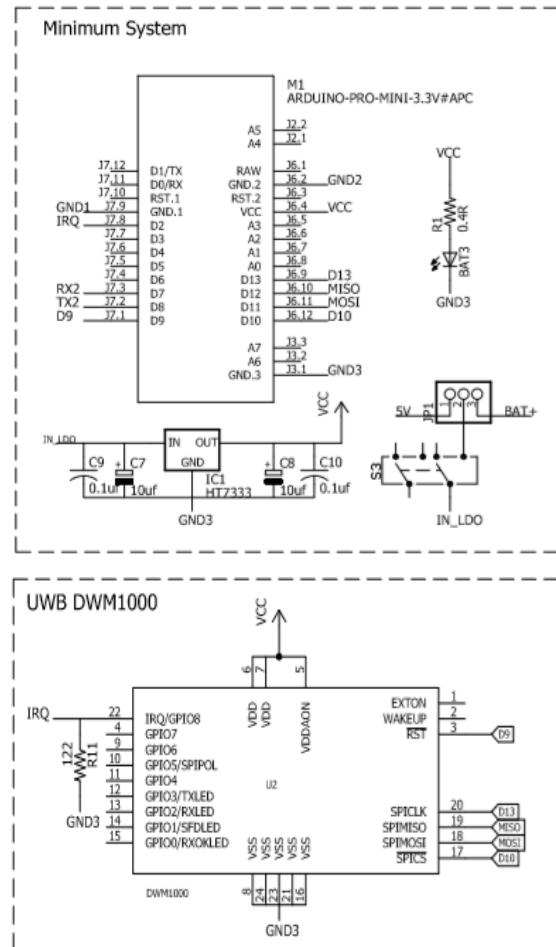


Figure 2. UWB tag and anchor schematic

B. UWB ranging algorithm

Figure 4 shows the ranging algorithm to measure distance between UWB tag and anchor. Measuring cycle is started when UWB tag transmit POLL message to idle UWB anchor. UWB anchor checks the message address. If the message address belongs to UWB anchor, UWB anchor transmits RANGE message to UWB tag. UWB tag receives RANGE message and checks the message address. If the message address belongs to UWB tag, UWB tag calculates the range.

UWB has several modes of range measurements algorithm. There are symmetrical single sided-two way ranging (SSS-TWR), symmetrical double sided-two way ranging (SDS-TWR) and asymmetrical double sided-two way ranging (ADS-TWR). We can choose the best algorithm with minimal error

$$SSS - TWR T_{prop} = \frac{T_{round} - T_{reply}}{2} \quad (1)$$

Figure 5 shows the SSS-TWR algorithm. In the SSS-TWR algorithm, UWB Device A transmits a message to UWB Device B. Then, UWB Device B receives the message and transmits the answer to UWB Device A. The time between the received message process and the transmitted answer process of UWB Device B is Treply. The time between the transmitted message process and the received

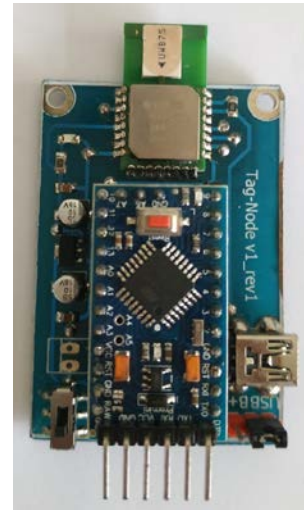


Figure 3. UWB tag and anchor transceiver

answer process of UWB Device A is Tround. Tprop is propagation ranging time. Tprop can be calculated by (1).

$$SDS - TWR T_{prop} = \frac{T_{round1} - T_{reply1} + T_{round2} - T_{reply2}}{4} \quad (2)$$

Figure 6 shows the illustration of SDS-TWR algorithm. In the SDS-TWR algorithm, UWB Device A transmits a message to UWB Device B. Then, UWB Device B receives the message and transmits the

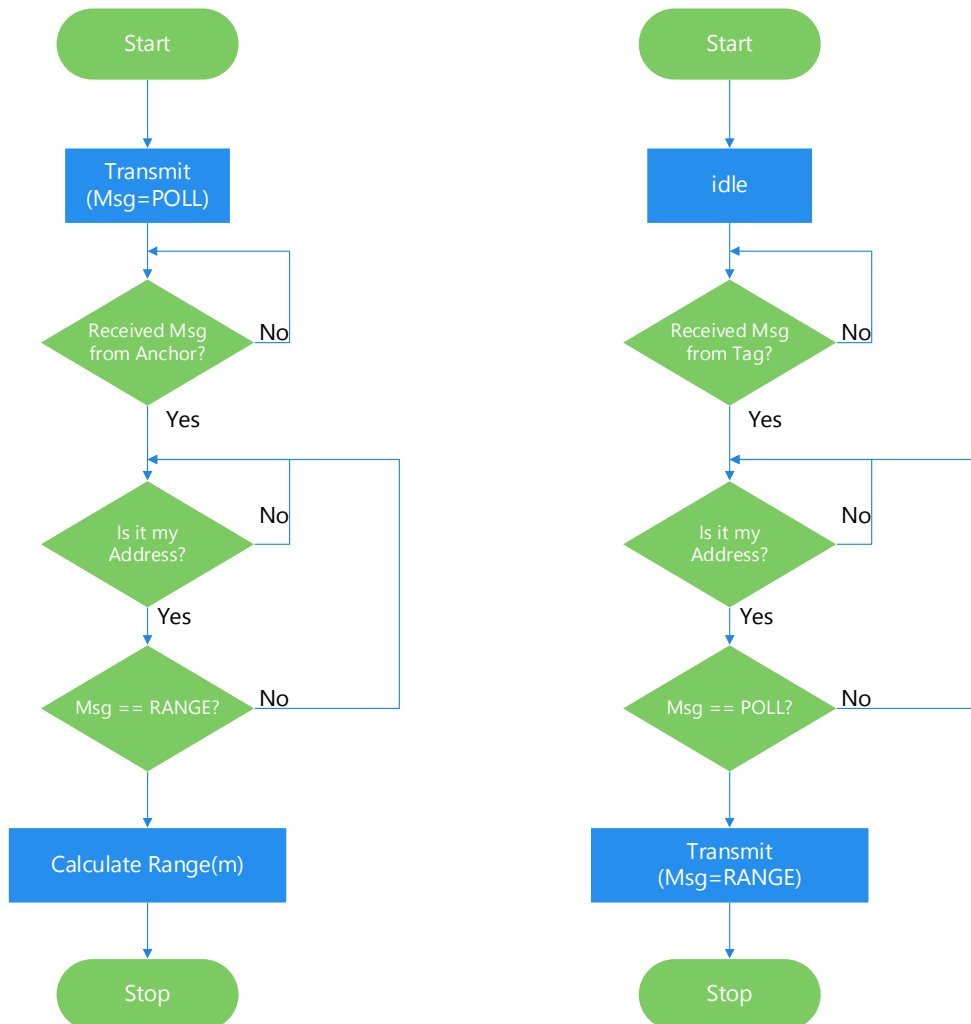


Figure 4. UWB ranging flowchart

answer to UWB device A. UWB device A receives answer and transmits it back to UWB device B. Tround1, Tround2, Treply1, and Treply2 are transmitting and receiving duration of UWB message, respectively.  $T_{prop}$  can be calculated by (2).

ADS-TWR illustration is same as SDS-TWR, but with different equation propagation time. Equation (3) shows ADS-TWR equation. This equation eliminates error when Treply1 and Treply2 have same value.

$$ADS - TWR T_{prop} = \frac{T_{round1} * T_{round2} - T_{reply1} * T_{reply2}}{T_{round1} + T_{round2} + T_{reply1} + T_{reply2}} \quad (3)$$

The distance between UWB tag and anchor can be calculated by (4)

$$\text{distance (meter)} = C * T_{prop} * t \quad (4)$$

where C is the light velocity (299792458 m/s),  $T_{prop}$  is the ranging propagation time of UWB, and t is the UWB resolution timestamp (~15.6 ps).

### C. Autonomous VTOL specification

This section presents about the autonomous VTOL specification. We continuously develop autonomous VTOL over three years for research and competition. We choose hexacopter configuration to improve the lift weight ability.

Figure 7 shows the autonomous VTOL. The autonomous VTOL used six brushless motors. UWB tag is attached above payload box to receive ranging data from UWB anchor. The payload box can carry seven boxes. Each box's maximum dimension and maximum weight are 10 cm x 10 cm x 4 cm and 100 gr—high-level and low-level controller centrally located on the frame. GPS is used when autonomous VTOL cannot detect UWB signal.

Figure 8 shows the block diagram of autonomous VTOL. The autonomous VTOL controller consists of a low-level controller and a high-level controller. The low-level controller uses hex cube Pixhawk 2.1 with redundant IMU and GPS. The main task of a low-level controller is flight navigation control system. The high-level controller uses ODROID mini pc. The high-level controller main task is additional custom algorithm processing by the user like image and video processing, including local positioning system. 433 radio transmitter is used to communicate with ground control software. Autonomous VTOL uses a 5000 mAh battery to get 10 minutes of flight time. This autonomous VTOL has been equipped with UWB Tag for local positioning. UWB tag sends ranging data to the high-level controller and calculates autonomous VTOL x, y position. The detailed calculation for the x, y position is described in the methodology.

### D. Method

This section presents about trilateration method to localize autonomous VTOL. This method is used to calculate UWB tag position. Figure 9 shows the trilateration model illustration. (x, y) is UWB tag position, and the position is moveable. UWB anchor has fix position. (x1, y1) is UWB anchor 1 position, (x2, y2) is UWB anchor 2 position, and (x3, y3) is UWB

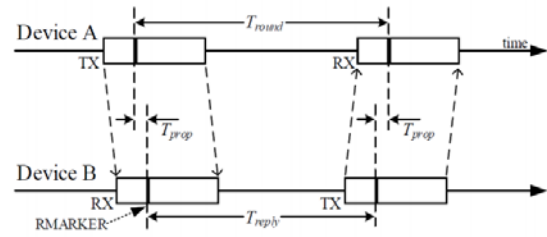


Figure 5. SSS-TWR range measurements mode algorithm

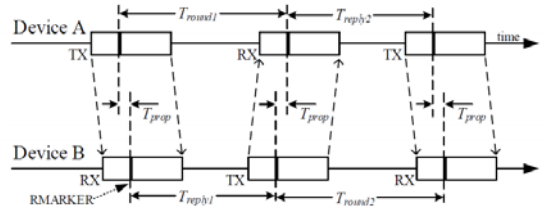


Figure 6. SDS-TWR range measurements mode algorithm



Figure 7. The hexacopter autonomous VTOL

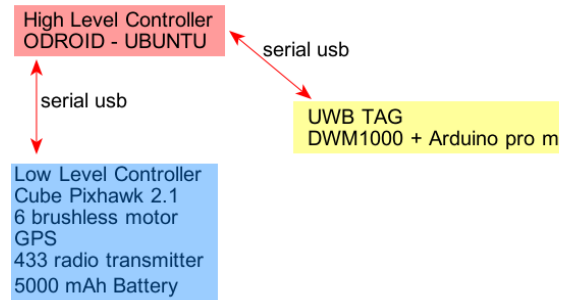


Figure 8. Autonomous VTOL block diagram

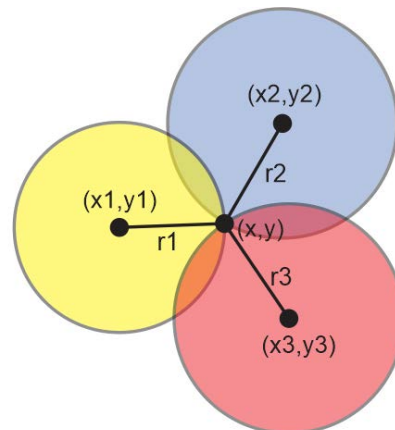


Figure 9. Trilateration model

anchor 3 position. Trilateration input is distance data between UWB tag and anchor ( $r_1, r_2, r_3$ ).

A circle with (x,y) coordinate has an equation:

$$x^2 + y^2 = r^2 \quad (5)$$

The trilateration equation for UWB Tag at (x, y) and UWB Anchor at ( $x_1, y_1$ ), ( $x_2, y_2$ ), and ( $x_3, y_3$ ) are:

$$(x - x_1)^2 + (y - y_1)^2 = r_1^2 \quad (6)$$

$$(x - x_2)^2 + (y - y_2)^2 = r_2^2 \quad (7)$$

$$(x - x_3)^2 + (y - y_3)^2 = r_3^2 \quad (8)$$

x is UWB tag x-axis position, y is UWB tag y-axis position.  $x_1, x_2$ , and  $x_3$  are UWB anchor 1, anchor 2, and anchor 3 x-axis fixed position.  $y_1, y_2$ , and  $y_3$  are UWB anchor 1, anchor 2, and anchor 3 y-axis fixed position.  $r_1$  is distance between UWB tag and anchor 1.  $r_2$  is distance between UWB tag and anchor 2.  $r_3$  is distance between UWB tag and anchor 3.

Then, equations (6), (7), and (8) can be further derived to (9), (10), and (11)

$$x^2 - 2x_1x + x_1^2 + y^2 - 2y_1y + y_1^2 = r_1^2 \quad (9)$$

$$x^2 - 2x_2x + x_2^2 + y^2 - 2y_2y + y_2^2 = r_2^2 \quad (10)$$

$$x^2 - 2x_3x + x_3^2 + y^2 - 2y_3y + y_3^2 = r_3^2 \quad (11)$$

Subtracting (9) by (11):

$$(-2x_1 + 2x_2)x + (-2y_1 + 2y_2)y = r_1^2 - r_3^2 - x_1^2 + x_2^2 - y_1^2 + y_2^2 \quad (12)$$

Then, subtracting (10) by (11):

$$(-2x_2 + 2x_3)x + (-2y_2 + 2y_3)y = r_2^2 - r_3^2 - x_2^2 + x_3^2 - y_2^2 + y_3^2 \quad (13)$$

Lets rewrite (12) using A,B,C values, and (13) using D,E,F values. This would in the following form:

$$Ax + By = C \quad (14)$$

$$Dx + Ey = F \quad (15)$$

Lets rewrite equation (14) and (15) into matrix (16)

$$\begin{bmatrix} A & B \\ D & E \end{bmatrix} \begin{bmatrix} x \\ y \end{bmatrix} = \begin{bmatrix} C \\ F \end{bmatrix} \quad (16)$$

$$\begin{bmatrix} x \\ y \end{bmatrix} = \begin{bmatrix} A & B \\ D & E \end{bmatrix}^{-1} \begin{bmatrix} C \\ F \end{bmatrix} \quad (17)$$

$$\begin{bmatrix} x \\ y \end{bmatrix} = \frac{1}{AE-BD} \begin{bmatrix} E & -B \\ -D & A \end{bmatrix} \begin{bmatrix} C \\ F \end{bmatrix} \quad (18)$$

$$\begin{bmatrix} x \\ y \end{bmatrix} = \frac{1}{AE-BD} \begin{bmatrix} EC & -BF \\ -DC & AF \end{bmatrix} \quad (19)$$

From (19), we can calculate x and y coordinate:

$$x = \frac{EC-BF}{AE-BD} \quad (20)$$

$$y = \frac{AF-DC}{AE-BD} \quad (21)$$

### III. Results and Discussions

In the first experiment, we conducted a distance ranging test for each UWB module. The main objective is to get maximum distance ranging ability and distance error measurement. Figure 10 shows the experimental setup of the UWB module. This

experiment was conducted to measure the distance between UWB tag and anchor. UWB anchor and computer is located in a fixed position. UWB tag was placed at a specific distance (1 m until 29 m). UWB Anchor calculated the distance to UWB Tag using SSS-TWR, SDS-TWR or ADS-TWR based radio signal. Then the calculated distance was sent to a computer.

This experiment compares symmetrical single sided-two way ranging (SSS-TWR), symmetrical double sided-two way ranging (SDS-TWR) and asymmetrical double sided-two way ranging (ADS-TWR) to get an accurate ranging measurement. Figure 11 shows UWB distance measurement using the SSS-TWR algorithm. The X-axis is the distance between UWB tag and anchor, and the y-axis is UWB anchor measurement value using the SSS-TWR algorithm. The result has been demonstrated that the UWB module can measure the maximum distance at 26.83 m. Figure 12 shows the error reading. The x-axis is the distance between UWB tag and anchor, and the y-axis is the percent error measurement value. In 1 m measurements, UWB gets 12 % error measurement or equal to 0.12 m. Then in 13 m measurement, UWB gets 2.3 % error measurement or equal to 0.299 m, and in 26 m measurement, UWB gets 0.69 % error measurement or equal 0.1794 m. The average error of symmetrical single sided-two way ranging algorithm is 2.73 %, the maximum error is 12.00 %, and the minimum error is 1.58 %.

Figure 13 shows UWB distance measurement using the SDS-TWR algorithm. The x-axis is the distance between UWB Tag and Anchor, and the y-axis is UWB Anchor measurement value using the SDS-TWR algorithm. The result has been demonstrated that the UWB module can measure the maximum distance at 28.99 m. Figure 14 shows error reading. The x-axis is the distance between UWB Tag and Anchor, and the y-axis is the percent error measurement value. In 1 m measurement, UWB gets 7.31 % error measurement or equal to 0.073 m. Then in 13 m measurement, UWB gets 1.20 % error measurement or equal to 0.1547 m, and in 26 m measurement, UWB gets 2.0 % error measurement or equal to 0.4732 m. Thus, symmetrical double sided-two way ranging (SDS-TWR) algorithm average error is 1.83 %, the maximum error is 7.31 %, and the minimum error is 0.64 %.

Figure 15 shows UWB distance measurement using the ADS-TWR algorithm. The x-axis is the distance between UWB tag and anchor, and the y-axis is UWB anchor measurement value using ADS-TWR algorithm. The result has been demonstrated that the UWB module can measure the maximum

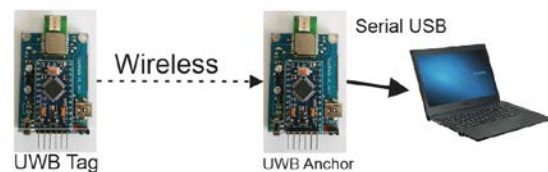


Figure 10. UWB transceiver distance ranging test set up

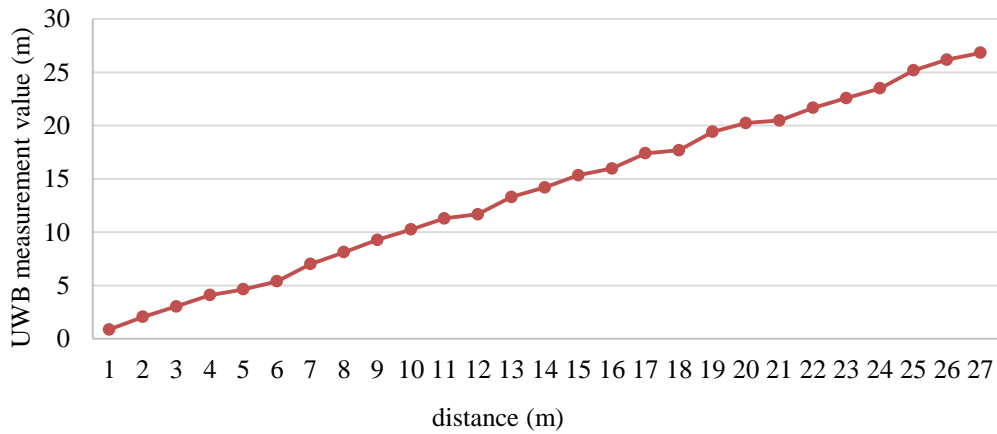


Figure 11. SSS-TWR measurement result

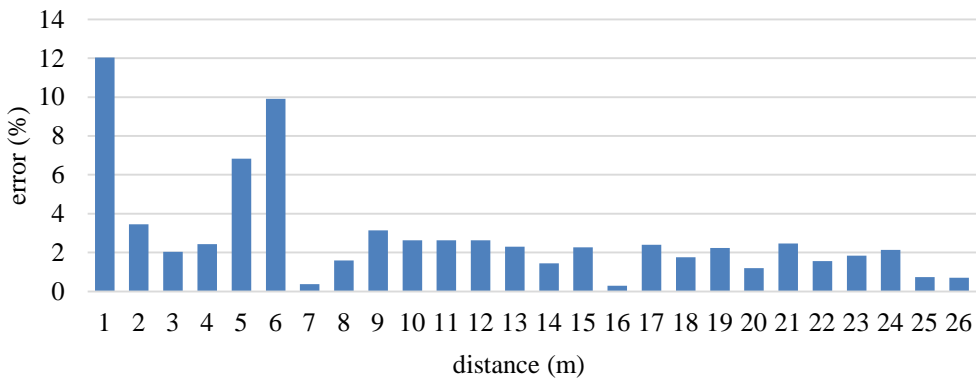


Figure 12. SSS-TWR distance measurement error

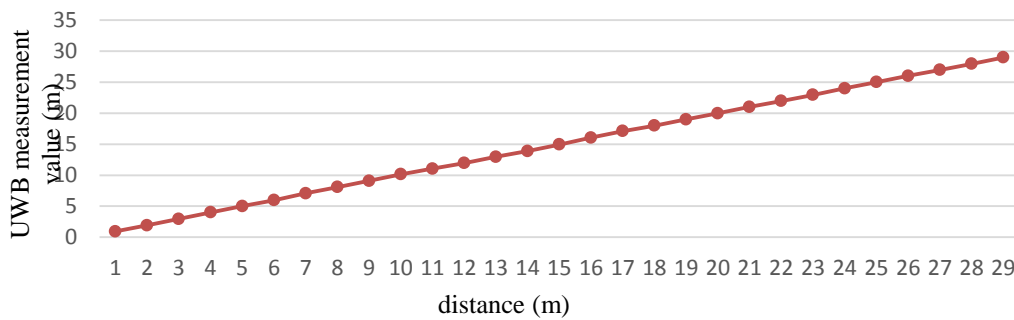


Figure 13. SDS-TWR measurement result

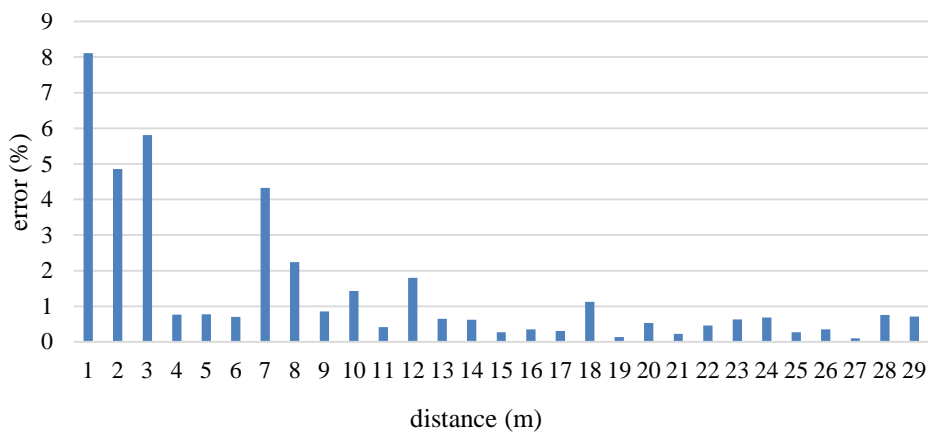


Figure 14. ADS-TWR distance measurement error

distance at 28.99 m. Figure 16 shows the error reading. In 1 m measurement, UWB gets 8.1 % error measurement or equal to 0.081 m. Then in 13 m measurement, UWB gets 0.64 % error measurement

or equal to 0.0832 m, and in 26 m measurement, UWB gets 0.34 % error measurement or equal 0.084 m. asymmetrical double sided-two way ranging (ADS-TWR) algorithm average error is

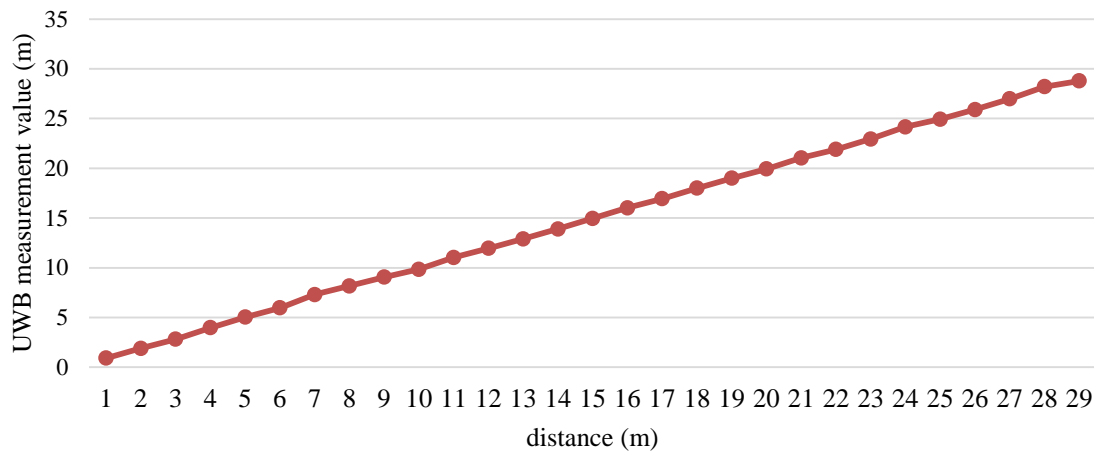


Figure 15. ADS-TWR measurement result

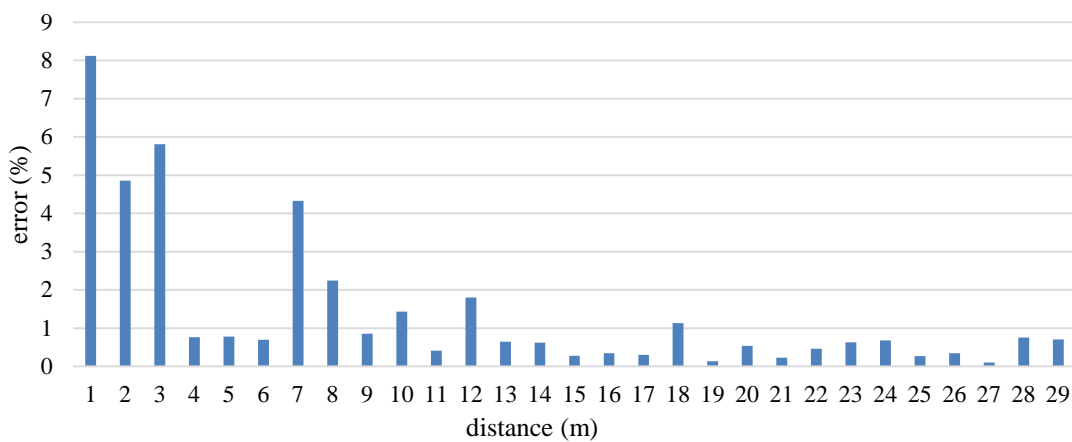


Figure 16. ADS-TWR distance measurement error

1.38 %, the maximum error is 7.31 %, and the minimum error is 0.64 %.

From the first experiment, ADS-TWR is superior to others by resulting in minimum distance error. ADS-TWR can measure longer distance than SSS-TWR and SDS-TWR. It also has minimal distance measurement error. ADS-TWR average error is 1.38 % (0.3588 m), SDS-TWR average error is 1.83 % (0.4758 m), SSS-TWR average error is 2.73 % (0.7098 m). The second experiment is UWB local positioning system implementation in autonomous VTOL using ADS-TWR ranging measurement method, and calculate the position of autonomous VTOL using trilateration method. Figure 17 shows the documentation of the second experiment when using autonomous VTOL hover. The orange area is dropping point. UWB tag is installed on autonomous VTOL, and UWB anchor is installed on a tripod. Figure 17 only shows +3 of 7 dropping points and 2 of 3 UWB anchors because the camera cannot capture all areas.

Figure 18 shows the autonomous VTOL flight path. This experiment was carried out in an outdoor area (20.00 m x 30.00 m). We used autonomous VTOL to drop seven payloads in a specific position. Home location position (red square, 3 m x 3 m) is (1.50, 1.50), and dropping positions (yellow square, 2 m x 2 m) are (8.50, 11.00), (1.00, 15.00), (4.00,

22.5), (1.00, 28.00), (18.50, 26.00), (12.50, 20.00), (17.00, 7.50). Initially, Autonomous VTOL took-off from home position (red square). Autonomous VTOL went to dropping point 1 and reached DROP 1 position, and then autonomous VTOL dropped the first payload successfully. Next, autonomous VTOL went to dropping point 2 and reached DROP 2 position, and then autonomous VTOL dropped the second payload successfully. Autonomous VTOL went to dropping point 3 and reached DROP 3 position, and then autonomous VTOL dropped the third payload successfully. Next, Autonomous VTOL went to dropping point 4 and reached DROP 4 position, and then autonomous VTOL dropped the fourth payload successfully. Autonomous VTOL went to dropping point 5 and reached DROP 5 position, and then autonomous VTOL dropped the fifth payload successfully. Next, Autonomous VTOL went to dropping point 6 and reached DROP 6 position, and then autonomous VTOL dropped the sixth payload successfully. Autonomous VTOL went to dropping point 7 and reached DROP 7 position, and then autonomous VTOL dropped the seventh payload successfully. Next, Autonomous VTOL went to the home point and successfully reached the HOME position, then autonomous VTOL land. This system can be used to localize the area for the dropping and landing of an autonomous VTOL.



Figure 17. Second experiment documentation

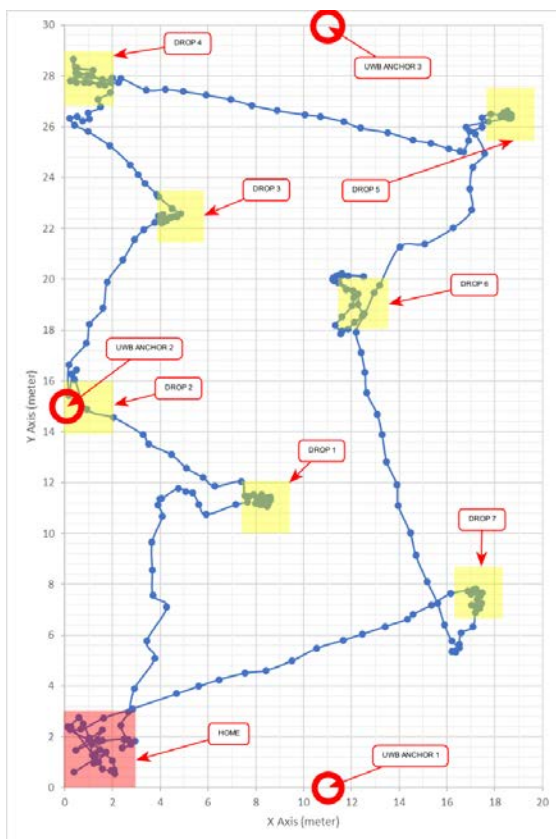


Figure 18. Recorded autonomous VTOL flight path using UWB system

#### IV. Conclusion

We have compared SSS-TWR, SDS-TWR, and ADS-TWR UWB ranging measurement modes. ADS-TWR can measure longer distance than SSS-TWR and SDS-TWR up to 29 m. ADS-TWR also has minimal distance measurement error. ADS-TWR average error is 1.38 % (0.3588 m), SDS-TWR average error is 1.83 % (0.4758 m), SSS-TWR average error is 2.73 % (0.7098 m). We also successfully implemented autonomous VTOL Quadcopter positioning in a small local outdoor area (20 m x 30 m). Autonomous VTOL has been able to drop seven payloads in seven areas (2 m x 2 m) and landed in the home position (3 m x 3 m) successfully.

#### Acknowledgement

This research was funded by research unit of Politeknik Elektronika Negeri Surabaya (PENS) to PENS multirotor research team. The authors would

like to thank PENS and PENS multirotor research team for supporting to publish this paper.

#### Declarations

##### Author contribution

All authors contributed equally as the main contributor of this paper. All authors read and approved the final paper.

##### Funding statement

This research did not receive any specific grant from funding agencies in the public, commercial, or not-for-profit sectors.

##### Conflict of interest

The authors declare no known conflict of financial interest or personal relationships that could have appeared to influence the work reported in this paper.

##### Additional information

Reprints and permission information is available at <https://mev.lipi.go.id/>.

Publisher's Note: Research Centre for Electrical Power and Mechatronics - Indonesian Institute of Sciences remains neutral with regard to jurisdictional claims and institutional affiliations.

#### References

- [1] S. Akahori, Y. Higashi, and A. Masuda, "Position estimation system with UWB, IMU and a distance sensor for quad-rotors," in *TENCON 2017 - 2017 IEEE Region 10 Conference*, pp. 1992–1996, 2017.
- [2] V. Mai et al., "Local Positioning System Using UWB Range Measurements for an Unmanned Blimp," *IEEE Robot. Autom. Lett.*, vol. 3, no. 4, pp. 2971–2978, 2018.
- [3] A. Ledergerber and R. D'andrea, "Calibrating Away Inaccuracies in Ultra Wideband Range Measurements: A Maximum Likelihood Approach," *IEEE Access*, vol. 6, pp. 78719–78730, 2018.
- [4] W. Guosheng, Q. Shuqi, L. Qiang, W. Heng, L. Huican, and L. Bing, "UWB and IMU System Fusion for Indoor Navigation," in *2018 37th Chinese Control Conference (CCC)*, 2018, pp. 4946–4950, 2018.
- [5] D. Feng, C. Wang, C. He, Y. Zhuang, and X.-G. Xia, "Kalman-Filter-Based Integration of IMU and UWB for High-Accuracy Indoor Positioning and Navigation," *IEEE Internet Things J.*, vol. 7, no. 4, pp. 3133–3146, 2020.
- [6] K. Ren, G. Bernes, M. Hetta, and J. Karlsson, "Tracking and analysing social interactions in dairy cattle with real-time locating system and machine learning," *J. Syst. Archit.*, vol. 116, p. 102139, 2021.
- [7] A. D. Ramadhani, P. Kristalina, and A. Sudarsono, "Performance Evaluation of Refinement Method in Indoor Localization," in *2018 International Electronics Symposium on Engineering Technology and Applications (IES-ETA)*, 2018, pp. 183–188, 2018.
- [8] R. Giuliano et al., "Indoor Localization System Based on Bluetooth Low Energy for Museum Applications," *Electronics*, vol. 9, no. 6, 2020.
- [9] M. Pušnik, M. Galun, and B. Šumak, "Improved Bluetooth Low Energy Sensor Detection for Indoor Localization Services," *Sensors*, vol. 20, no. 8, 2020.
- [10] S. Cheng, S. Wang, W. Guan, H. Xu, and P. Li, "3DLRA: An RFID 3D Indoor Localization Method Based on Deep Learning," *Sensors*, vol. 20, no. 9, 2020.
- [11] R. D. Ainul, P. Kristalina, and A. Sudarsono, "Hybrid filter scheme for optimizing indoor mobile cooperative tracking system," *Telkomnika (Telecommunication Comput. Electron. Control)*, vol. 16, no. 6, pp. 2536–2548, 2018.
- [12] C. Zhang, N. Qin, Y. Xue, and L. Yang, "Received Signal Strength-Based Indoor Localization Using Hierarchical Classification," *Sensors*, vol. 20, no. 4, 2020.

- [13] I. Ashraf, S. Hur, S. Park, and Y. Park, "DeepLocate: Smartphone Based Indoor Localization with a Deep Neural Network Ensemble Classifier," *Sensors*, vol. 20, no. 1, 2020.
- [14] S. Monica and F. Bergenti, "An Algorithm for Accurate and Robust Indoor Localization Based on Nonlinear Programming," *Electronics*, vol. 9, no. 1, 2020.
- [15] P. Ssekidde, O. Steven Eyobu, D. S. Han, and T. J. Oyana, "Augmented CWT Features for Deep Learning-Based Indoor Localization Using WiFi RSSI Data," *Appl. Sci.*, vol. 11, no. 4, 2021.
- [16] P. Li, X. Yang, Y. Yin, S. Gao, and Q. Niu, "Smartphone-Based Indoor Localization With Integrated Fingerprint Signal," *IEEE Access*, vol. 8, pp. 33178–33187, 2020.
- [17] T. Koike-Akino, P. Wang, M. Pajovic, H. Sun, and P. V Orlik, "Fingerprinting-Based Indoor Localization With Commercial MMWave WiFi: A Deep Learning Approach," *IEEE Access*, vol. 8, pp. 84879–84892, 2020.
- [18] X. Peng, R. Chen, K. Yu, F. Ye, and W. Xue, "An Improved Weighted K-Nearest Neighbor Algorithm for Indoor Localization," *Electronics*, vol. 9, no. 12, 2020.
- [19] H. S. Maghdid, K. Z. Ghafoor, A. Al-Talabani, A. S. Sadiq, P. K. Singh, and D. B. Rawat, "Enabling accurate indoor localization for different platforms for smart cities using a transfer learning algorithm," *Internet Technol. Lett.*, vol. n/a, no. n/a, p. e200.
- [20] S. Sadowski, P. Spachos, and K. N. Plataniotis, "Memoryless Techniques and Wireless Technologies for Indoor Localization With the Internet of Things," *IEEE Internet Things J.*, vol. 7, no. 11, pp. 10996–11005, 2020.
- [21] S. Ranade and P. V Manivannan, "Quadcopter Obstacle Avoidance and Path Planning Using Flood Fill Method," in *2019 2nd International Conference on Intelligent Autonomous Systems (ICoIAS)*, pp. 166–170, 2019.
- [22] W. Hönig, J. A. Preiss, T. K. S. Kumar, G. S. Sukhatme, and N. Ayanian, "Trajectory Planning for Quadrotor Swarms," *IEEE Trans. Robot.*, vol. 34, no. 4, pp. 856–869, 2018.
- [23] J. Shen, S. Wang, Y. Zhai, and X. Zhan, "Cooperative relative navigation for multi-UAV systems by exploiting GNSS and peer-to-peer ranging measurements," *IET Radar, Sonar & Navig.*, vol. 15, no. 1, pp. 21–36, 2021.
- [24] F. Gu, S. Valaee, K. Khoshelham, J. Shang, and R. Zhang, "Landmark Graph-Based Indoor Localization," *IEEE Internet Things J.*, vol. 7, no. 9, pp. 8343–8355, 2020.
- [25] I. Ashraf, M. Kang, S. Hur, and Y. Park, "MINLOC: Magnetic Field Patterns-Based Indoor Localization Using Convolutional Neural Networks," *IEEE Access*, vol. 8, pp. 66213–66227, 2020.